Title of your IAU Symposium
Proceedings IAU Symposium No. 363, 2022
A.C. Editor, B.D. Editor & C.E. Editor, eds.

DOI: 00.0000/X000000000000000X

PULXs as Accreting Magnetars: Observational Manifestations

Nabil Brice[1], Silvia Zane[1], Roberto Taverna[2], Roberto Turolla[2,1], Kinwah Wu[1]

[1]Mullard Space Science Laboratory, University College London, Holmbury St. Mary, Dorking, Surrey, RH5 6NT, UK

[2]Department of Physics and Astronomy, University of Padova, via Marzolo 8, 35131Padova, Italy

Abstract. Pulsating Ultra Luminous X-ray sources (PULXs) are thought to be X-ray bright, accreting, magnetized neutron stars, and could be the first and only evidence for the existence of magnetars in binary systems. Their apparent soft (< 20 keV) X-ray luminosity can exceed the Eddington luminosity for a neutron star (NS) by a few orders of magnitude. Although several scenarios have been proposed to explain the different components observed in the X-ray spectra and the characteristics of the X-ray lightcurve of these system, detailed quantitative calculations are still missing. In particular, the observed soft X-ray lightcurves are almost sinuosidal and show an increase in the pulsed fraction (from 8% up to even 30%) with increasing energy. Here, we present how emission originating from an optically thick envelope, expected to be formed during super-Eddington accretion, can result in pulsed fractions similar to observations.

1. Introduction

PULXs are point-like X-ray bright sources with apparent luminosities $> 10^{39}$ erg s^{-1} in the $0.1 - 20$ keV energy band, which is above the Eddington luminosity for a $1.4M_{\odot}$ object (at $\sim 3 \times 10^{39}$ erg s^{-1}). The physical mechanism that produces a super-Eddington luminosity is still debated, although there are two main candidate scenarios. One possible scenario is a luminosity amplification due to geometric beaming (King & Lasota 2019). Another promising scenario is super-Eddington accretion onto a neutron star (NS) with a magnetar-like magnetic field, which would allow for sufficient opacity reduction to increase the maximum luminosity (Mushtukov *et al.* 2015; Brice *et al.* 2021).

One crucial observational property of PULXs is an almost sinusoidal pulse, which was first discovered in M82 X-2 (Bachetti *et al.* 2014). Sinusoidal pulses were also observed in the PULXs NGC7793 P13 (Fürst *et al.* 2016; Israel, Papitto *et al.* 2017) and NGC5907 ULX1 (Israel, Belfiore *et al.* 2017) For all these sources, the shape of the observed pulsed profile does not change dramatically with the energy, except for the fact that the pulsed fraction increases with increasing energy , e.g. for NGC5907 ULX1 going from $\sim 12\%$ for < 2 keV to $\sim 20\%$ for > 7 keV (Israel, Belfiore *et al.* 2017).

Previously, it was shown by Mushutkov *et al.* (2021) that pulsed fractions $\gtrsim 20\%$ make interpretations with a strong luminosity amplification (such as that needed to explain the apparent luminosity of NGC5907 ULX1) unlikely. However, no similar study has been done on the maximum pulsed fraction from an optically thick envelope formed by super-Eddington accretion.

A study of the super-Eddington accretion scenario was conducted by Mushtukov *et al.* (2017), who find that an optically thick envelope is formed when there is a sufficiently large ($\gtrsim 10^{19}$g s^{-1}) mass accretion rate. However, the observational manifestations of an optically thick envelope were not studied in detail. The aim of the work presented

here is to study the pulsed fraction and phase-averaged spectrum from an accreting NS system with an optically thick envelope and compare with the measurements obtained for PULXs.

2. Model

In the typical scenario of accretion onto a highly magnetised NS, the accretion disc is truncated at the magnetospheric radius

$$R_m \approx 7 \times 10^7 \Lambda \; M^{1=7} R_6^{10=7} B_{\mathrm{d};12}^{4=7} L_{39}^{-2=7} \mathrm{cm}, \tag{2.1}$$

where Λ is a dimensionless parameter that depends on the mode of accretion (typically $\Lambda = 0.5$ for accretion via thin disc), M is the mass of the NS in units of solar mass, R_6 is the radius of the NS in units of 10^6 cm, $B_{\mathrm{d};12}$ is the dipole field strength in units of 10^{12}G, and L_{39} is the accretion luminosity in units of 10^{39}erg s^{-1}. In addition, the disc penetrates some finite distance, P_m, into the magnetosphere. The values for P_m are not well known.

In the region where the disc penetrates into the magnetosphere, which is bounded by the magnetic field lines that reach out to R_m and $R_m - P_m$ (see figure 1), the accreting material is channelled along the magnetic field lines to the magnetic polar caps. For mass accretion rates $\gtrsim 10^{19}$g s^{-1}, the channelled material is optically thick and so an optically thick envelope surrounds the NS.

Since the disc does not penetrate the magnetosphere to the NS surface, the optically thick envelope surrounds an empty cavity (that includes the NS). Radiation emitted from the accretion column is then injected into the cavity and becomes thermalised due to multiple scatterings off the envelope walls. The envelope walls re-radiate to the exterior as a multicolour blackbody, with the temperature at each point on the wall dependent on the optical depth of the wall (assuming grey atmosphere scattering).

The optical depth, τ, of each point along the envelope wall depends on the dynamics of the accretion flow and the shape of the bounding magnetic funnel. We model the dynamics of the flow as charges moving along the magnetic field lines, subject to gravitational and centrifugal forces. We solved the equations of motion analytically to obtain the velocity at any specified coordinate along the magnetic field line: (θ, φ). Together with a description of the geometry of the funnel, we can obtain the optical depth $\tau(\theta)$.

Following Mushtukov *et al.* (2017), we assume scattering through a grey atmosphere, hence the temperature on the outer wall, T_{out}, is related to the blackbody temperature in the cavity, T_{in}, via

$$T_{\mathrm{out}} = \tau^{-1=4} T_{\mathrm{in}}. \tag{2.2}$$

2.1. *Ray-tracing*

Once a temperature map of the envelope walls is obtained, we calculated the phase-dependent spectra by ray-tracing the emitting envelope point to an observer at infinity, along a particular line-of-sight direction, while accounting for shadowing by the envelope and by the disc. We used an adapted IDL code from Taverna & Turolla (2017), which calculates the phase and energy-dependent spectra of a fireball trapped by dipole magnetic field lines close to the surface. We adapted the IDL code to account for the emission and shadowing from a thin planar disc and for envelopes formed from magnetic field lines reaching farther from the surface than in the trapped fireball case.

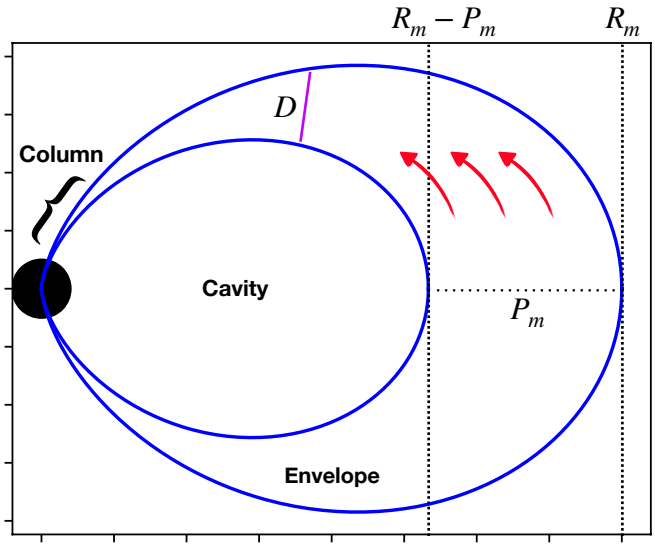

Figure 1. A cartoon of the model set-up of the optically thick envelope. Two bounding magnetospheric field lines are shown in blue. The larger and smaller arcs show dipole field lines reaching out to radii R_m and $R_m - P_m$ respectively. The purple line shows an example, for a particular latitude, of the shortest path along which the radiation diffuses outward and is labelled by the distance D. The black circle represents the surface of the NS. The red arrows show the accretion flow.

The pulsed fraction is calculated using the phase-dependent flux F:

$$\mathrm{PF}_\Delta = \frac{F_{\Delta;\mathrm{max}} - F_{\Delta;\mathrm{min}}}{F_{\Delta;\mathrm{max}} + F_{\Delta;\mathrm{min}}}, \tag{2.3}$$

where Δ specifies some energy interval over which the specific flux is integrated, and max (min) indicate taking the maximum (minimum) over the rotation phase.

The phase-averaged spectrum of a particular model is calculated from averaging the phase-dependant spectrum over the rotation phase. We analysed the phase-averaged spectra by fitting to a blackbody plus blackbody spectral model.

3. Application to NGC 7793 P13

For comparison of the synthetic spectra with real spectra, we considered the analysis done by Koliopanos *et al.* (2017) of the *XMM-Newton* observation of NGC 7793 P13 (obs. 0748390901), in the $0.1-10$keV energy band. We used the inferred X-ray luminosity from the same observation and spin period of the source as fixed model parameter inputs.

We estimated the dipole magnetic field strength model parameter, B_d, by calculating models for various values of B_d and comparing the black-body temperatures from the fitting of the synthetic spectra with the temperatures of the MCD plus black-body fit of the observed spectrum. We used the value of B_d that resulted in the closest match between synthetic and observed spectra.

Figure 2 shows the pulsed fraction calculated from the synthetic spectra of models with various tilt angles of the magnetic dipole moment with respect to the spin axis, λ, and a distribution of observer line-of-sight angles with respect to the spin axis, χ. We fixed the input model parameters: luminosity, spin period, and dipole magnetic field strength

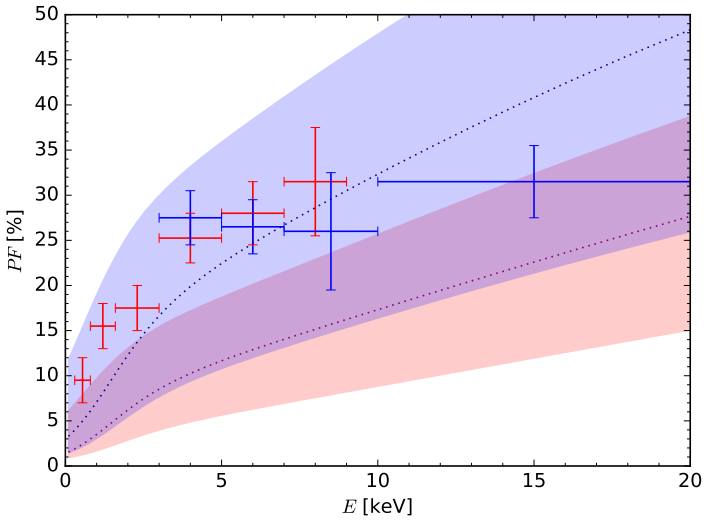

Figure 2. Pulsed fraction as a function of energy. The red and blue points with error bars are the observed *XMM-Newton* and *NuSTAR* data, respectively, reported by Fürst *et al.* (2016). The light blue and light red shaded regions indicate the range of pulsed fraction values obtained by varying the value of χ (from $\chi = 12$ for the dashed line at the bottom to $\chi = 68$ for the solid line at the top). The light blue and light red area are for models with a tilt angle of $\lambda = 8$ and $\lambda = 4$, respectively.

as described previously. For comparison of the pulsed fraction obtained from the synthetic spectra and the measured pulsed fraction of the source, we considered the analysis done by Fürst *et al.* (2016) of *XMM-Newton* observations and *NuSTAR* observations. We found that models with $\lambda \approx 8°$ and $\chi \approx 25 - 35°$ are capable of producing the observed pulsed fraction and the increasing trend with energy, at least up to ~ 10 keV. Our models overestimate the pulsed fraction at high energies (i.e. the value measured from the *NuSTAR* data in the $10 - 20$ keV band). This may be indicative of a high energy, unpulsed, emission component of the spectrum, which is not accounted for in our simple envelope plus disc scenario.

NB acknowledges STFC for support through a PhD fellowship.

References

Bachetti M., et al. 2014 *Nature*, 514, 202
Brice N., Zane S., Turolla R., Wu K. 2021 *MNRAS*, 504, 701
Fürst F., et al. 2016, *APJ*, 831, L14
Israel G. L., Belfiore A., et al. 2017 *Science*, 355, 6327
Israel G. L., Papitto A., et al. 2017, *MNRAS*, 466, L48
King A., Lasota J. 2019 *MNRAS*, 485, 3588
Koliopanos F., Vasilopoulos G., Godet O., Bachetti M., Webb N. A., Barret D. 2017, *A&A*, 608, A47
Mushtukov A. A., Portegies Zwart S., Tsygankov S. S., Nagirner D. I., Poutanen J. 2021, *MNRAS*, 501, 2424
Mushtukov A. A., Suleimanov V. F., Tsygankov S. S., Ingram A. 2017, *MNRAS*, 467, 1202
Mushtukov A. A., Suleimanov V. F., Tsygankov S. S., Poutanen J. 2015, *MNRAS*, 454, 2539
Taverna, R., & Turolla, R. 2017, *MNRAS*, 469, 3610